Heike M. Herold and Thomas Scheibel*

Applicability of biotechnologically produced insect silks

DOI 10.1515/znc-2017-0050
Received March 23, 2017; revised June 29, 2017; accepted June 30, 2017

Abstract: Silks are structural proteins produced by arthropods. Besides the well-known cocoon silk, which is produced by larvae of the silk moth *Bombyx mori* to undergo metamorphosis inside their silken shelter (and which is also used for textile production by men since millennia), numerous further less known silk-producing animals exist. The ability to produce silk evolved multiple independent times during evolution, and the fact that silk was subject to convergent evolution gave rise to an abundant natural diversity of silk proteins. Silks are used in air, under water, or like honey bee silk in the hydrophobic, waxen environment of the bee hive. The good mechanical properties of insect silk fibres together with their non-toxic, biocompatible, and biodegradable nature renders these materials appealing for both technical and biomedical applications. Although nature provides a great diversity of material properties, the variation in quality inherent in materials from natural sources together with low availability (except from silkworm silk) impeded the development of applications of silks. To overcome these two drawbacks, in recent years, recombinant silks gained more and more interest, as the biotechnological production of silk proteins allows for a scalable production at constant quality. This review summarises recent developments in recombinant silk production as well as technical procedures to process recombinant silk proteins into fibres, films, and hydrogels.

***Corresponding author: Thomas Scheibel,** Lehrstuhl Biomaterialien, Fakultät für Ingenieurwissenschaften, Universität Bayreuth, Universitätsstraße 30, 95440 Bayreuth, Germany, E-mail: thomas.scheibel@bm.uni-bayreuth.de; Bayreuther Zentrum für Kolloide und Grenzflächen (BZKG), Universität Bayreuth, Universitätsstraße 30, 95440 Bayreuth, Germany; Bayreuther Zentrum für Molekulare Biowissenschaften (BZMB), Universität Bayreuth, Universitätsstraße 30, 95440 Bayreuth, Germany; Institut für Bio-Makromoleküle (bio-mac), Universität Bayreuth, Universitätsstraße 30, 95440 Bayreuth, Germany; Bayreuther Materialzentrum (BayMAT), Universität Bayreuth, Universitätsstraße 30, 95440 Bayreuth, Germany; and Bayerisches Polymerinstitut (BPI), Universitätsstraße 30, 95440 Bayreuth, Germany
Heike M. Herold: Lehrstuhl Biomaterialien, Fakultät für Ingenieurwissenschaften, Universität Bayreuth, Universitätsstraße 30, 95440 Bayreuth, Germany

Keywords: biomedical applications of silks; biotechnological silk production; recombinant insect silks; silk inspired materials; silk processing.

1 Introduction

Silk – no other fabric has fascinated mankind so intensely over the millennia. The light weight combined with the smooth touch and shiny appearance surrounded the fabric with an aura of splendour and luxury ever since. Due to the admiration silk earned, its production was fiercely contested. Wild silk-producing moths could be found in many places, but collecting enough of the wild moths was strenuous and resulted in low production rates. The Chinese were the ones to solve this problem through sericulture, i.e. the rearing of silkworms for the production of silk. Domestication of the moth *Bombyx mori* (*B. mori*) in the Neolithic time, together with ongoing development of silk purification and processing methods, allowed China to dominate the silk business. The detailed knowledge on how to create high-quality silk fabrics from the silkworms' cocoon was kept secret over centuries and therefore generated a great export trading volume, which even gave the name to the ancient network of trade routes that connected the Asian and the European continents, the so-called Silk Road. To date, sericulture is an important industrial sector in China, and China continues to produce the largest quantity of raw silk worldwide [1].

Humans exploited the unique properties of silk materials not only for precious cloth. The extraordinary mechanical properties of spider silk, i.e. its high extensibility combined with great strength, allowed the use of silk threads for various tools. For example, fishing nets were created by wrapping spider webs around pronged, wooden branches. Moreover, the military used silk threads for thin, precise, and durable cross hairs [2]. Together with the low immunogenicity of some silks, this material is also suitable for use in biomedical applications. Civilisations as early as ancient Romans and Greeks used spider silk webs to stop bleedings or to cover wounds [3]. Later, silk fibres were also used as suture material [4].

1.1 Silk-producing insects

Silks are extracorporeal structural materials produced by arthropods. Even though the focus of sericulture clearly lays on the moth *B. mori*, and silkworm and spiders are the most prominent producers of silk, many silk-producing animals can be found in the classes of Insecta, Arachnida, and Myriapoda [5]. Typically, they use silk for shelter, reproduction, foraging, or dispersal. In many cases, the pupation cocoons of holometabolous insects (i.e. insects that undergo complete metamorphosis) are produced from this proteinaceous material. Additionally, evolution gave rise to the use of silk for several other purposes. Midges may live in aquatic tubes lined with silk threads, and mayflies line their U-shaped burrows in submerged wood with silk. Crickets bind leaves together to construct cocoon-like nests, dragonflies anchor their eggs to vegetation, and lacewings protect their eggs on silken egg stalks. Caddisfly larvae build nets to fish prey under water, and silverfish use silk to transfer sperm. A comprehensive summary of the use of silks in the class of Insecta is given in reference [6].

The great diversity of silks is partly owed to the fact that they are a result of convergent evolution, i.e. silks have been "invented" multiple times during evolution. Based on the phylogenetic relationship, the method of production, and the dominant silk structure, as many as 23 silk lineages in 17 orders have been proposed, with each lineage likely depicting an independent evolutionary event [6]. Whilst the overall diversity of silks is abundant, typically, one individual insect species mainly produces one type of silk [5]. Only in Neuroptera the production of several types of silk has been reported [7]. For example, the larvae of the green lacewing (*Mallada signata*) produce a predominantly α-helical cocoon silk protein to spin a loosely woven cocoon for pupation [7], whereas adult lacewings produce a completely different, unrelated egg stalk silk composed of (cross) β-structure [8]. This contrasts most spiders, which typically produce several types of silk. One example is the European garden spider *Araneus diadematus*. Individuals of these species produce up to seven types of silk for different purposes: tough silk with high tensile strength to build the frame of the orb web or a highly elastic silk to construct the catching spiral and other silk types to wrap caught prey or to protect eggs [9]. According to the respective use of the silk, different silks vary greatly in their mechanical properties (see Table 1). Especially spiders have evolved silks with extraordinary mechanical properties in order to catch prey, which are normally insects in mid-flight, as it is necessary to withstand the enormous kinetic impact of flying insects on the web [11, 12].

Taken together, silks represent a very heterogeneous material in both structure and function. However, they share some common features. Silken materials are based on proteins rich in alanine, serine, and glycine residues; the proteins are stored as highly concentrated solutions (silk dope) in specialised glands; they solidify in a spinning process often associated with shear forces [5] and, upon solidification, fold into a single dominant secondary structure resulting in mechanically strong and/or tough fibres [6]. Whilst the majority of spider silk proteins are rather of high molecular weight comprising a highly repetitive core domain with various sequence motifs to ensure proper folding during solidification, insect silks are often of smaller size and exhibit a less repetitive character.

1.2 Molecular structure of silk

From a molecular point of view, silks typically contain high amounts of the amino acid residues glycine, serine, and alanine. This is most likely attributable to their non-essential character, i.e. silk production is mostly independent from nutrition. Additionally, silks need to be

Table 1: Comparison of mechanical properties of silk fibres and synthetic fibres.

Material	Strength (MPa)	Extensibility (%)	Toughness (MJ/m³)
Honey bee silk (*A. mellifera*)	132	204	–
Lacewing egg stalk silk (*C. carnea*) (70% rel. humidity)	155	210	87
Caddisfly silk	33	126	17
Silkworm silk (*B. mori*)	600	18	70
Spider silk – dragline (*A. diadematus*)	1100	27	160
Nylon fiber	950	18	80
Kevlar 49 fiber	3600	2.7	50
Carbon fiber	4000	1.3	25
High-tensile steel	1500	0.8	6

Table reprinted with permission from [10].

soluble even at high protein concentrations as found in silk glands but, at the same time, need to allow for the formation of stable fibres, the solid state. Therefore, an intermediate hydrophobicity as provided by these amino acid residues seems favourable [6].

Silks are semicrystalline materials. They consist of ordered, crystalline structures embedded in an amorphous matrix. Five silk types have been identified based on the dominant structural element found in different silks: coiled-coil, extended β-sheet, cross-β sheet, collagen triple helix, and polyglycine II. Although there are tremendous differences between the individual primary and secondary structures of the proteins, the regularity within one type of silk structure allows tight packing of the protein and the formation of an extended network of hydrogen bonds forming intra- as well as inter-protein chain connections [6]. The crystallite regions exhibit a high hydrogen bond density and account for the strength of the fibre, whilst entanglement of chains within the unordered regions with less hydrogen bond density account for the flexibility. Although the mechanical properties of silk fibres rely largely on the huge network of hydrogen bonds, further stabilizing mechanisms may occur, including crosslinking of protein chains by covalent bonds via disulphide bridges, as seen in the connection of heavy-chain (H chain) and light-chain (L chain) protein of *B. mori* fibroin.

The silk of silkworms, that of related moths, and the web silk of orb-weaving spiders (the latter discussed here briefly, due to their importance, although spiders are not a member of the class of Insecta) share some features. Their silk proteins often comprise a high molecular weight, and whilst the termini are rather hydrophilic, the repetitive core is composed of alternating large hydrophobic blocks interspersed with short hydrophilic spacers. Strikingly, the core domains form β-sheet crystallites during processing into solid fibres [13]. Their primary sequences consist of repeats of very explicit motifs to ensure proper folding of the β-strand and to further allow multiple stacking of strands to form extended β-sheet structures. Alternating amino acid side chains facing opposite sides of the sheet have to be well-conserved to ensure similar size and hydrophobicity of the interacting residues [6]. The hydrophobic domains of *B. mori* H chain contain GX repeats with X being alanine, serine, threonine, or valine residues and form predominantly antiparallel β-sheets, which contribute to the mechanical properties of the fibres [14]. Motifs such as GAGAGS also occur. Spider dragline silks are composed primarily of two different protein classes, MaSp1 and MaSp2 (major ampullate spidroin 1 and 2) [15]. Both protein classes exhibit hydrophobic poly-alanine stretches accounting for β-sheet crystallites, which are aligned along the fibre axis and which contribute to the high tensile strength of spider silk fibres. Less organised hydrophilic blocks interrupt the crystallite structures, with motifs such as GGX forming presumably 3_{10} helices in MaSp1 or GPGXX forming β-turn spirals in MaSp2 (with X being typically tyrosine, leucine, or glutamine), both imparting elasticity to the protein fibre. Beta strands can also align into cross β-sheets, where β-strands of similar length are interrupted by β-turns, which allow antiparallel arrangement, and the β-sheet structures are aligned perpendicular to the fibre axis [6]. Naturally occurring cross β-sheets are rare, but they have been described in lacewing egg stalks [8], in capture threads of glow worms [16], in egg-raft silk of water-beetles [16], and in weevil cocoons [17].

A very special and unusual insect silk is produced by silverfish. During mating, male grey silverfish of the species *Ctenolepisma longicaudata* produce a silk that is used as a tactile stimulus. Besides low molecular orientation, low aqueous stability, and an atypical amino acid composition, remarkably, the secondary structure of this silk is characterised by high contents of random coil structures with only some amount of β-sheet structures. Instead of a dominant crystalline secondary structure providing extensive hydrogen bonding within ordered crystallites to stabilise the fibres, entanglement of the protein chains was identified as the major mechanism to cohere the proteins into a solid material [18].

Larvae of bees, ants, and hornets produce cocoon silks with tetrameric coiled-coil structures running parallel to the fibre axis to undergo metamorphosis [16, 19, 20]. Coiled-coil is a widely spread structural motif where multiple helices wind around each other to prevent hydration of hydrophobic residues buried in the core of the structure. The underlying proteins are characterised by a primary structure revealing seven-residue periodicity, the so-called heptad repeats, denoted as $(abcdefg)_n$, usually containing hydrophobic residues in the *a* and *d* positions and hydrophilic residues in the remaining positions [21]. The amino acid composition of the coiled-coil silks revealed an unusual high content of alanine, a small hydrophobic amino acid, in the entire coiled-coil sequence but particularly in the *a* and *d* core position [20, 22], whereas most known coiled-coil proteins contain mainly large hydrophobic residues, such as leucine and isoleucine, in these positions in order to increase the hydrophobic forces stabilising the structure [21]. Whilst the reduced coiled-coil stability in solution might be compensated by the high protein concentrations found in the silk glands, the presence of the comparatively small amino acid residues found in the core explained the smaller than expected superhelix radius of the four-stranded coiled-coil structure, as

residues such as alanine allow a tighter packing of the helices. Notably, to some extent, polar amino acid residues, such as serine, are found in positions *a* and *d* as well [20]. Comparison of several coiled-coil silk proteins revealed a lower degree of sequence identity among different species, which might be a result of recurring amino acid substitutions with amino acids revealing similar properties, thereby not interfering with the assembly into the coiled-coil structure. The general character of the side chains seems to be more important than the precise evolutionary conservation of the exact sequence; therefore, the sequence of these heptad repeats allows variations to some extent [22].

Additionally, silks with a collagen-like triple helical structure exist. The amino acid chain folds into a left-handed helix with three amino acids per turn. Three of these helices assemble to form a right-handed superhelix that runs parallel to the fibre axis. Every third amino acid residue is located inside the helix core, but solely glycine residues with hydrogen as side chain are allowed in this position due to sterical reasons. Further, silks with a polyglycine II lattice structure show similar features as collagen helices. The proteins in polyglycine II structures consist of consecutive glycine residues, which fold into a right-handed helix whereby several helices arrange into hexagonal arrays [6]. It is speculated whether silks with collagen-like structure have evolved from polyglycine structures, as only minor exchanges were required. Silks with polyglycine II structure are produced by some Allantinae, Heterarthrinae, and Blennocampinae species, whilst related collagen-like structures are present in the cocoons of animals from the tribe Nematini as well as in species from the Blennocampinae and Tenthredininae [6].

Studies concerning the correlation of silk structure, silk glands in which the silk is produced, and the final function of the silk revealed no substantial connection between them; all types of silk protein structure can be produced in labial glands, and they are produced for a huge variety of functions [6]. Further, whilst the β-sheet silks of Lepidoptera are used for many different applications, cocoons of different insect groups are constructed from all types of silk protein structures [6]. The fact that there is no direct correlation between silk production gland, structure, and function points towards the hypothesis that silks are to some extent interchangeable [6].

2 Natural silk processing

Organisms in the 23 different silk-producing insect lineages all have to handle the conversion of the highly concentrated liquid silk dope into a solid (fibrous) material [23]. The silk proteins undergo solidification in most cases whilst being drawn from the gland into the extracorporeal environment. The spinning process must be highly controlled to ensure a reliable fibre formation to bestow the required mechanical properties of the fibre. At the same time, premature solidification inside the gland or the duct must be prevented. Understanding the natural spinning process is necessary to overcome the challenge of producing man-made silk fibres with mechanical properties comparable to fibres produced by spiders or insects.

The spinning process is often initiated by the fixation of a silk fibre to a surface. The orifice connecting the fixed silk with the silk gland is pulled away inducing a silk stream starting from the gland where the spinning dope is stored to deliver material for the fabrication of the solid silk fibre. Alternatively, a silk dope can be deposited on a surface and "spun" into a fibre in the extracorporeal environment as seen in e.g. lacewings. Female lacewings produce silken egg stalks to protect their offspring from predators. Subsequent to silk secretion onto a surface, an egg is dipped in, and the abdomen together with the egg is pulled away [24]. Thereby, a thin egg stalk is created on top of which the egg resides. A few seconds later, the egg stalk is hardened and the egg can be released completely. In either way, the process of spinning can be regarded as pultrusion rather than extrusion, as the fibres are drawn by force from the gland rather than being pushed [23]. Cohesive forces, such as inter- and intramolecular hydrogen bonds as well as entanglement of amorphous regions, prevent capillary breakup of the stream and ensure interruption-free fibre production.

Although this type of fibre spinning is elegant in its simplicity, more elaborate processes have evolved to meet the variety of requirements imposed to the fibres. The natural spinning process has been studied most thoroughly in the silk glands of silkworms [25]. A number of factors have been reported to influence the fibre formation, including variations in pH (Figure 1), salt concentration, silk protein concentration, and shear forces along the gland conferring solubility to the silk proteins in the silk gland whilst inducing formation of inter- and intramolecular connections during solidification of the silk [26]. First, the silk protein is synthesised in the posterior region of the gland and secreted into the gland's lumen [27]. Here, the highly soluble protein is concentrated up to 15 wt% (weight percent) and forms micelles with the hydrophilic termini pointing towards the micelle surface, whilst hydrophobic residues are buried inside the micelles. As the proteins proceed through the middle gland towards the spinneret, the solution is acidified and the silk proteins are further concentrated up to

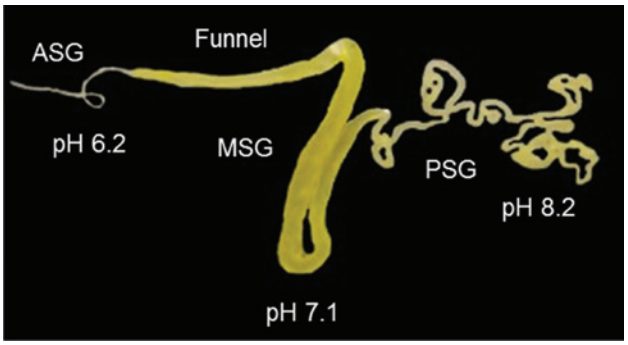

Figure 1: Silk gland of *B. mori*. pH values are indicated in different parts of the silk gland.
ASG, anterior silk gland; MSG, middle silk gland; PSG, posterior silk gland. Reprinted and adapted from [13] under Creative Common Licence.

30 wt% for storage [28]. The micelles are thought to condense into globular structures, and the solution is further acidified in the anterior silk gland. Using pH-sensitive dyes, a pH drop from approximately 6.9 in the posterior silk gland to 4.8 in the anterior silk gland has been reported [29]. More recently, using a concentric ion selective microelectrode, a gradient from pH 8.2 from the posterior silk gland to 6.2 in the beginning of the anterior silk gland (the very anterior region was not accessible for the electrodes) has been reported [30]. Salts are added to the spinning dope, and shear forces applied by the spinneret lead to the formation of water-insoluble fibres. The solidification process occurs under major structural transitions into the final β-sheet structure. The sericin, which envelopes the fibre, is thought to dehydrate the dope and to further promote the transition from liquid to solid state [23].

The amino terminal domain of fibroin heavy chain is highly important for fibre assembly. At neutral pH, the domain shows a random coil structure. Acidic residues prevent dimerisation of the domain via charge repulsion. Upon acidification, the side chains are protonated and enable the formation of homodimers. The importance of this mechanism is further underlined by the finding that the residues involved in the inhibition of premature dimer formation are conserved in Lepidoptera and Trichoptera [31, 32]. In general, silk processing in silk glands of spiders shows similarities to the process in silkworms. The protein solutions are highly concentrated, a drop in pH induces oligomerisation of the spidroins controlled by the terminal domains (which reveal five helix bundles in the case of spider silk proteins [33, 34]), and ions are added prior to the final fibre formation [35].

Rheological measurements revealed that native spinning dopes of spider dragline and silkworm cocoon silk proteins show many similarities although they evolved separately; both dopes are visco-elastic with properties of typical polymer melts with high viscosities [36, 37]. Such a material in principle could challenge the animals due to the relatively high forces needed for processing. However, liquid crystal structures have been observed in silk ducts of spider and silkworm silk glands, which disappear right before the dope enters the spinneret [38, 39]. These structures reduce inter-molecular friction resulting in a lower viscosity and thereby reducing the energetic effort of spinning a fibre. The shear thinning behaviour of silk dopes is well characterised and is in accordance with findings that creating fibrillar structures from silk dope demands three orders of magnitude less work compared to that from polymer melts not forming liquid crystalline structures [40].

Silks of the cocoon of *B. mori* or the dragline silks of Araneidae generally comprise flexible proteins of high molecular weight with amphipathic character, which allows them to form large, micelle-like mesogens (liquid crystal forming units) in solution and, at the same time, to solidify into β-sheet crystallite containing structures upon mechanical stress. These β-sheet forming silks are referred to as "canonical silks" by Walker et al. [23].

In contrast to these canonical silks, "non-canonical" silk proteins contain other types of secondary structures and are typically short and exhibit a rod- or lath-like structure. It is proposed that the fibre formation process in these silks differs dramatically from that of canonical silks as their crystallites might act as both mesogens and crystallites [23]. For example, in the glands of honey bee larvae, birefringent structures, the so-called tactoids, are ingrained in an isotropic fluid and can already be detected in the silk gland. They were reported to be first located near the surface of the silk-secreting cells and later in the entire gland lumen [41, 42]. These tactoids exhibit a regular banding pattern pointing towards the existence of fused tactoids forming a cohesive mesophase. Moreover, a structure called fibrous bars has been described in silk glands of bumblebees and hornets [41], which might correspond to the mesophase structure. During the solidification process, no major structural transition occurs, as the folded mesogenic proteins show the same structural content as the crystallites in the solid silk [23].

3 Recombinant silk protein production

Although the mechanical properties of silks as well as their biocompatibility have been well known for millennia, the

variation in quality inherent in materials from natural sources together with the low availability (except from *B. mori* silk) impeded the development of applications of silks. In recent years, recombinant silks have attracted interest as the biotechnological production of silk proteins allows for a scalable production at constant quality. For the heterologous silk gene expression, several different expression hosts have been utilised, like yeasts, mammalian cell lines, insect cells, and even transgenic animals and plants [43]. However, bacteria, such as *Escherichia coli* (*E. coli*), can be regarded as the preferred expression host, as a plethora of suitable expression plasmids as well as different engineered strains are well established. Commonly, recombinant gene expression is associated with the cloning of a DNA sequence encoding the desired protein into an expression vector, and upon transformation of a suitable expression host with the vector, the respective protein can be produced by the host. Subsequent purification steps then yield the desired protein.

Unfortunately, for many silk proteins, the genetic sequence encoding the protein is unknown or only partially known, and therefore, the identification of silk gene and protein sequences is of high interest. To identify silk sequences, most commonly, mRNAs are obtained from silk glands. However, many insects do not produce silks throughout the entire lifespan. For example, the silk glands of *B. mori* are larva-specific tissues, which even degenerate shortly after pupation in a process of programmed cell death, which is precisely controlled by hormones, such as 20-hydroxyecdysone (20E) and juvenile hormone (JH) [44–46]. Although silkworms constantly produce a certain amount of silk proteins, large amounts of silk protein are produced by the last instar to produce cocoons [47]. Therefore, often the final instar larvae are investigated for silk gene expression. As RNA is prone to degradation, the RNA isolated from silk glands is transcribed into cDNA. The emerging cDNA library, therefore, only contains the exons of the respective genes. In order to identify silk sequences, the transcriptome obtained from the cDNA library analysis is matched with genome sequences and further with mass spectrometry pattern obtained from tryptic digestion of proteins present in the silk gland. Based on homologies, silk sequences of closely related silk-producing insects can be identified and thereby accelerate the knowledge on silk sequences.

To produce recombinant proteins, original or codon optimised gene sequences can be cloned into an expression vector, and expression hosts can be exploited to produce the protein. Especially for the production of small, non-repetitive insect silk proteins, *E. coli* has been shown to be a suitable host. In contrast, the production of high molecular weight silk proteins as found in silkworms (or spiders) encounters a size limit of well-expressible genes in bacterial hosts resulting in the production of fragmented silk proteins caused by premature transcriptional or translational termination events, further impaired by depletion of specific tRNAs upon a bias in codon usage of different species, i.e. gene donor and expression host. Repetitive gene sequences may further undergo homologous recombination leading to shortening of the genetic information and consequently of the encoded protein [43]. For the recombinant production of these proteins, different expression hosts have to be chosen or the genetic sequence has to be adapted to the bacterial expression host concerning codon usage and size limitations, for example, by derivation of consensus sequences from reoccurring sequence stretches.

A major benefit of recombinant production of silk proteins is the possibility to modify silk sequences on the genetic level according to the desired application. Incorporation of amino acid sequences is feasible, such as the well-known RGD motif for enhanced cell-silk interactions or amino acids providing functional groups for subsequent chemical modification of the silk protein.

3.1 Bee silk

Some small silk proteins are readily producible in bacterial hosts. One example is the coiled-coil silk of honey bees (*Apis mellifera*). In their larval stage, these bees produce a silken cocoon composed of four small and non-repetitive fibrous proteins of 30–34 kDa to undergo metamorphosis [48]. The underlying small genes (approximately 1 kbp) have been identified, and the respective cDNA was cloned into pET expression vectors to produce full-length proteins AmelF1-4 (*A. mellifera* fibroin 1–4) in *E. coli* Rosetta. Due to the small protein sizes, good yields of up to 2.5 g/l of ferment were obtained [49]. Interestingly, homologous sets of four silk encoding genes have been reported for other animals, e.g. bumblebees, bulldog ants, weaver ants, hornets, and Asiatic honeybees [22, 50, 51]. This is attributed to multiple gene duplication events in the precursor of the Aculeata [52]. Cloning of *Apis cerana* silk genes using primers, which amplify the respective silk genes without their signal peptides, allowed heterologous gene expression. The *E. coli* strain BL21 (DE3) served as expression host and enabled efficient protein production of ABS1-4 (Asiatic honey bee silk protein 1–4) with yields up to 60 mg/ml. The four main components of fibrous proteins of the cocoon produced by the larva of the yellow hornet *Vespa simillima* served as blueprints for

recombinant full-length proteins Vssilk1–4 (*Vespa simillima* silk 1–4) (34–46 kDa) [50]. The isoelectric points of the proteins produced in *E. coli* were determined to be 8.9, 9.1, 5.0, and 4.2, respectively [51], whilst the predicted isoelectric points of the ~30-kDa silk proteins of the giant honeybee *Apis dorsata* ranged from 5.0 to 5.9 [52]. The conservation of the four silk genes implies the importance of all four encoded proteins for either silk fabrication or function [53]. However, the amino acid composition of each set of proteins is similar and therefore might be, to some extent, redundant. It could be shown that materials made of one single recombinant honey bee protein mimics the properties of multi-protein silk materials and, therefore, can simplify the recombinant production of honey bee silk [53]. The production and analysis of recombinant silk proteins, therefore, not only are beneficial concerning the availability of protein but also enable the production and characterisation of single-silk materials made of, e.g. honey bee or hornet silk, which do not exist as such in nature.

3.2 Lacewing silk

A recombinant lacewing egg stalk protein, $N[AS]_8C$ based on one of the two dominant egg stalk proteins of the green lacewing *M. signata*, MalXB2, was designed for heterologous production in *E. coli* [54]. Eight repeats of a 48-amino-acid-long consensus motif of the MalXB2 core domain flanked by terminal domains are the basis for the 53-kDa engineered protein.

3.3 Silkworm silk

Notwithstanding the great availability of silkworm cocoon silk, the large size of the underlying proteins, and their repetitive character, approaches for the heterologous expression of *B. mori* silk genes in bacterial expression hosts have been developed. Natural silkworm fibroin is composed of heavy chain fibroin with a molecular weight of 350 kDa forming a complex with the 25-kDa light chain via a disulphide bridge [55, 56]. Recombinant production of full-length silkworm fibroin in *E. coli* has been reported but resulted in massive sequence deletions [57]. Therefore, to mimic the silk fibroin, synthetic silk-like proteins based on structural motifs but with adapted protein size were designed and produced in bacterial hosts. Prevalently, the amino acid sequence GAGAGS derived from the crystalline fibroin domain was integrated into rationally designed hybrid proteins, and this approach allowed an investigation of the influence of ratios of crystalline-to-amorphous moieties.

3.4 Artificial silk

Silk-elastin-like proteins (SELPs) are a family of recombinant block copolymers with repeated units of silk-like blocks (GAGAGS) and elastin-like blocks (GVGVP) putatively combining the high tensile strength of silk and the excellent resilience of elastin in one protein. The blocks can be defined by the general formula $([S]m[E]n)o$, where S is a silk block and E is an elastin block, m ranges usually from 2 to 8, n ranges from 1 to 16, and o ranges from 2 to 100, chosen with respect to n and m to yield a final protein polymer with an appropriate molecular weight, which is well-expressible by the envisioned expression host [58]. The blocks may be substituted depending on the desired properties of the final material, or single amino acids may be exchanged, e.g. in the elastin-like block. In the GXGVP motif, X often is valine but can be replaced by any amino acid residue except for proline, as it influences the coacervation of elastin [59, 60]. One commonly used SELP is SELP47-K. The 69.8-kDa protein consists of a monomer structure of $[S]_4[E]_4[EK][E]_3$, with EK being the pentapeptide sequence GKGVP with a lysine residue replacing one of the valine residues of the E module [58]. A great variety of combinations of silk blocks and elastin blocks exist, e.g. the 65.4-kDa protein SELP815K, which comprises eight silk units and 15 elastin units plus one lysine substituted elastin unit per monomer [61].

4 Morphologies of processed recombinant silk proteins and their putative application

With the rapidly expanding knowledge of natural silk fabrication, it became possible to develop a plethora of technical procedures to process recombinant silk proteins into man-made fibres. Going beyond the naturally occurring morphology of fibres, silk proteins can also be processed artificially into different morphologies, like films, particles, capsules, hydrogels, foams, or sponges. From a technical point of view, silk proteins can be regarded as polymeric materials with the exception that polymers are commonly processed from melt rather than from solution. For silk, differential scanning calorimetry (DSC) and thermogravimetric analysis (TGA) revealed a bimodal melting

and thermal decomposition as the temperature of melting and decomposition lie close together [62–64], making a processing from melt almost impossible. Therefore, silks are generally processed from organic or aqueous solutions [10]. In the following, a few selected morphologies and the respective processing as well as putative applications of recombinant silk proteins will be described in more detail.

4.1 Fibres and nonwoven mats

4.1.1 Methodologies

There are several methods to produce fibres from silk solutions. A rather simple method is drawing fibres from concentrated silk solution by hand. Closed tweezers can be dipped in a droplet of spinning dope, and by opening the tweezers, a fibre is formed. To some extent, this method even mimics the natural process of lacewings to produce egg stalks (Figure 2A).

In wet spinning, an aqueous or organic silk solution is extruded into a coagulation bath typically comprising aqueous kosmotropic salt solutions or polar organic solvents such as monohydric alcohols, i.e. methanol, ethanol, acetone, propanol, or isopropanol [65] (Figure 2B). It is the most commonly used fibre-spinning method for the production of artificial silk fibres in the micrometre range and leads to the production of single fibres. Depending on silk solvent and composition of the coagulation bath, mechanical properties of the fibre can be fine-tuned. As the fibre formation process progresses comparatively slow, it allows a high degree of alignment of the proteins and arrangement of the crystalline structures within the fibre [66]. Post-stretching has been shown to induce a higher alignment along the fibre axis and, therefore, can lead to improved mechanical properties [67].

Microfluidic spinning has been used to produce silk fibres by mimicking the geometry of the natural spinning apparatus and the flow profile (Figure 2C). This system allows alteration of the flow conditions of the silk solution, and by addition of sheath fluids, a pH drop can be induced or kosmotropic salts can be added.

Electrospinning is a technique in which an electrostatic field is applied to a slowly extruded solution to produce fibres in the micro- to nanometre range [68]. Typically, fast-evaporating chemicals are used as solvents. Whilst the solution is extruded through a nozzle, it is charged with high voltage. The potential difference between the charged polymer droplet and the counter electrode ideally causes a Taylor cone at the tip of the nozzle. As soon as the electrical attraction of the charged molecules overcomes the surface tension of the solvent, a fine jet is emitted given that the solution possesses a sufficiently strong cohesion (otherwise, a spray emits). Whilst migrating to the counter electrode, the solvent evaporates, and fibres deposit on the collector chaotically in the form of a non-woven mat [69] (Figure 2D). Depending on the electrospinning parameters, the characteristics of the produced fibre mat can be controlled. For example, by using a rotating collector, aligned fibres can be produced [70]. Adaption of parameters of the spinning dope, such as concentration, viscosity, conductivity, as well as of processing parameters such as voltage, distance to counter electrode, or humidity allows to control the fibre diameter [68]. This method of fibre production has attracted great interest for applications especially in the field of biomedicine, for example, as a scaffold material for cells in tissue regeneration, as the morphology of nonwovens mimics many naturally occurring structures, like collagen fibrils in the extracellular matrix, which have diameters around 40–150 nm. However, as the use of fast-evaporating solvents such as hexafluoroisopropanol (HFIP) is commonly

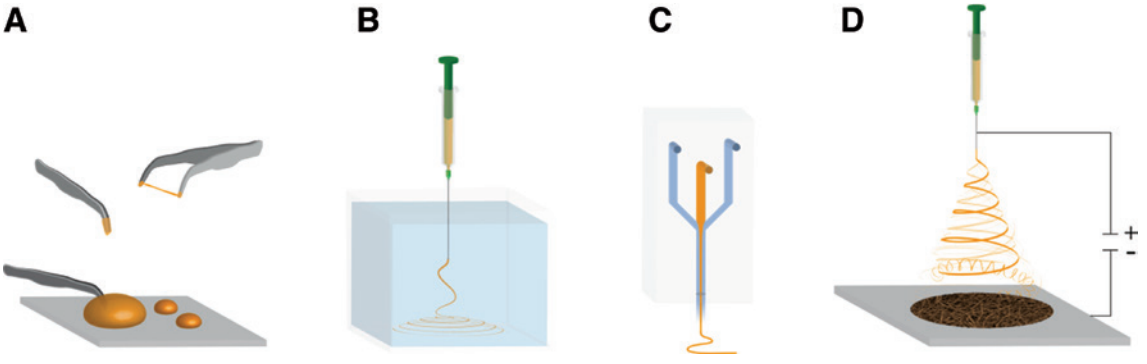

Figure 2: Illustration of different fibre-spinning methods.
(A) Hand drawing. (B) Wet spinning. (C) Microfluidic spinning. (D) Electrospinning.

Table 2: Mechanical properties of recombinant honey bee silk fibres.

	Diameter (μm)	Breaking stress (MPa)	Breaking strain (%)	True breaking stress (MPa)
"As-spun" fibres	30 ± 5	15 ± 3	225 ± 10	50 ± 12
Post-treated fibres	13 ± 7	150 ± 39	47 ± 26	213 ± 63
Native fibres	9	132	204	400

Data for "as-spun" fibres: strongest three out of six fibres tested; for post-treated fibres: strongest 10 of 21 fibres tested. Table adapted from [49].

required for electrospinning, electrospun fibres often show reduced mechanical properties for β-sheet crystallite silks compared to that of other processing methods, as the electric field interacts with hydrogen bond dipoles in the protein and thereby stabilises α-helical structures leading to reduced β-sheet formation and hampering proper alignment of the crystallites [71].

4.1.2 Examples

In order to analyse the fibre-forming properties of recombinant honey bee silk, aqueous solutions of AmelF1-F4 were prepared and concentrated using polyethylene glycol (PEG) dialysis [49]. Solutions containing only one of the proteins started to precipitate at 2–4% (w/v), and no fibres could be drawn from these low concentrations. Strikingly, equimolar mixtures containing all four proteins were stable up to 10–15% (w/v) (underlining their importance in nature), and fibres could be produced from this silk dope by hand drawing. Analysis of the secondary structure revealed a proportion of approximately 59% of coiled-coil structure in the artificial silk fibre, which is very similar to the 65% of coiled-coil structure found in native honey bee silk. Unexpectedly, these fibres were not birefringent, suggesting that the fibres were not aligned, although native honey bee silk fibres are aligned. Nonetheless, to render the fibres water insoluble, the fibres were submerged in methanol and post-stretched. This post-treatment caused strong birefringence of the fibres indicating alignment of the proteins within the fibre during this process. However, upon methanol treatment, a change in secondary structure from coiled-coil to β-sheet caused a drop of the coiled-coil proportion to 48%. Mechanical analysis of the hand-drawn fibres before and after post-treatment revealed that the ("as-spun") hand-drawn fibres initially had similar extensibility to native honey bee fibres and, at the same time, lower tensile strength, whilst post-treatment led to reduced extensibility but increased tensile strength (Table 2).

Besides recombinant honey bee silk, recombinant lacewing egg stalk silk has been processed into fibres by hand drawing [54]. The engineered 53-kDa protein $N[AS]_8C$ was dissolved in hexafluoroacetone (HFA) at concentrations of 10% (w/v); fibres were drawn and, after a drying step, post-treated at 60 °C and 70% relative humidity (RH). Analysis of the secondary structure showed that artificial egg stalks had a slightly lower content of β-sheet structure compared to natural ones. However, upon stretching of the fibres, the β-sheet content of the artificial egg stalks rose to the level of natural egg stalks. Tensile tests conducted with natural egg stalks revealed a high dependency of the mechanical properties on the RH [72]. The natural system responds to an increase in humidity by an increase of extensibility and strength and, therefore, in toughness. Tensile tests of the artificial egg stalks were conducted both at 30% and at 70% RH. Results revealed similar mechanical properties of the artificial egg stalks compared to the natural egg stalks of the common lacewing *Crysopa carnea* at 30% relative humidity; however, the artificial egg stalks showed only little dependency of extensibility and toughness on RH and could not compete with the extraordinary mechanical properties of the natural ones at 70% RH (Table 3).

Wet-spun fibres have been produced from the recombinant honey bee protein AmelF3 [73]. Concentrated aqueous silk solutions of around 10% protein content (containing sodium chloride and SDS) were extruded continuously through a needle into a methanol coagulation bath followed by a second methanol bath where the fibres were stretched. To render the fibres more stable, the dried fibres were heated for 1 h to 190 °C to induce covalent crosslinking, e.g. of glutamic acid residues with lysine residues to form a ε-(γ-glutamyl)-lysine isopeptide [74]. The produced fibres showed a diameter of ~34 μm with mechanical strength at break of 158 MPa and strain at break of 42% (in comparison to native honey bee silk with 132 MPa and 200% engineered stress and strain, respectively [75]). Although minor proportions of β-sheet structures are present in honey bee silk, native honey bee silk as well as aqueous solutions of the recombinant AmelF3 show predominantly helical structures. Upon wet spinning and fibre formation by coagulation into monohydric alcohols, the α-helical proportion was reduced from 43% to 31%,

Table 3: Mechanical properties of natural egg stalks of *C. carnea* and artificial egg stalks of $N[AS]_8C$.

	Extensibility (%)	Strength σ_{max} (MPa)	Young's modulus (MPa)	Toughness (MJ m^{-3})
Natural egg stalk				
30% RH	2±1	68±19	5777±1257	1.2±0.72
70% RH	210±100	155±75	3175±1016	87±49
Artificial egg stalk				
30% RH	5±2	55±14	2330±850	1.76±0.9
70% RH	6±3	25±11	1012±252	1.09±0.59

Table adapted from [54]. All experiments were carried out at 22 °C, at variable relative humidity (RH).

whilst the proportion of the emerging dominant structure of β-sheet rose to 36% as revealed by Raman spectroscopy [73]. Further investigations using polarised Raman spectroscopy unveiled that post-stretching of the fibres did not significantly alter the proportion of the respective secondary structures but led to an alignment thereof. Strikingly, whilst the helical structures were only moderately aligned in parallel to the fibre axis, a significant change in alignment was reported for β-sheet structures; they became highly aligned, strikingly, in perpendicular orientation to the fibre axis reminiscent to cross β-structures. This phenomenon was attributed to the geometry of the β-sheet crystallites [73]. As the molecular units will orientate in the direction of draw with the longest dimension of the crystallite parallel to the drawing force, i.e. the fibre axis, this allowed the implication that the crystallites are deeper than the sheets are wide, a structure that is also seen for lacewing egg stalk silk. Due to the flexibility of the produced fibres, these could be processed by weaving and knitting (Figure 3), which offers a high potential for diverse biomedical as well as technical applications. The possibility to modify the genetic sequence of the protein by substitution with other amino acids (containing functional groups) will allow further chemical modifications.

Wet spinning has been reported of the recombinant silk-elastin-like protein SELP-47K into micron-scaled fibres with high tensile strength and deformability [76]. Protein at 25% (w/v) was spun from formic acid into a methanol coagulation bath, and the resulting fibres were post-stretched during fibre collection. SEM analysis showed fibres with smooth surfaces and diameters in the range from less than 10 μm to over 60 μm. Concerning the secondary structure of the fibres, β-strand structures dominated the fibre with coexisting β-turn as well as β-sheet conformations. Antiparallel β-sheets were attributed to the silk-like blocks, although they were segregated by the elastin-like blocks. The mechanical properties of the resulting fibres were strongly dependent on the hydration state. Dried fibres exhibited a breaking elongation of less than 2% and an ultimate tensile strength of 20–80 MPa, which is lower than, e.g. in silkworm silk. The mechanical properties were referred to the elastin moiety of the fibre as elastin, which is very brittle in dry state. In contrast, elastin is very elastic when hydrated. Hydrated SELP-47K fibres exhibited greater strain to failure but a dramatically reduced tensile strength of about 1 MPa. Cross-linking the proteins with glutaraldehyde increased the ultimate tensile strength, for some fibres, up to 20 MPa, and strain to failure reached several hundred percent whilst the deformability was not compromised, offering the possibility to process these fibres into fabrics suitable for tissue engineering. Therefore, SELP-47K was spun from formic acid and post-treated with methanol, glutaraldehyde, or a combination of both [77]. Whilst FTIR measurements

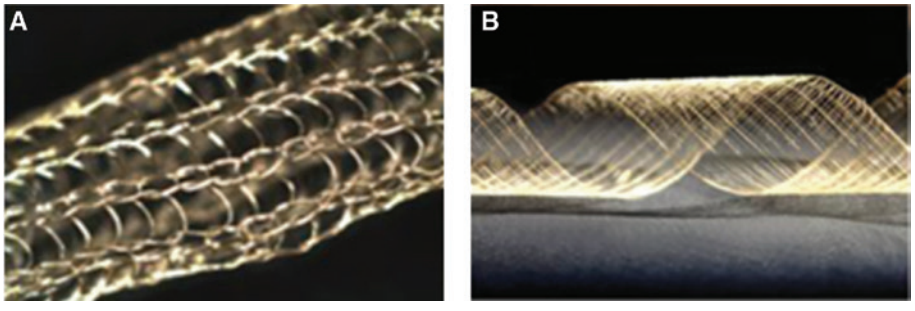

Figure 3: Wet-spun recombinant honeybee silk.
(A) Knitted into a tube. (B) Woven into a sheet. Reprinted and adapted with permission from [73].

of untreated scaffolds showed primarily β-turns and unordered conformations, antiparallel β-sheets emerged upon post-treatment. Fibroblasts adhered, spread, and remained viable on the scaffold, indicating that the non-woven mesh could be a promising material for biomedical applications (Figure 4). To further evaluate the potential of SELPs for the development of a mechanically robust tissue scaffold, as needed, e.g. for human vein and artery replacements, mechanical tests were carried out in the fully hydrated state of the fibre. Tensile tests of fibres fully submerged in phosphate-buffered saline (PBS) revealed elastic moduli of 3.4–13.2 MPa, an ultimate tensile strength of up to 13.5 MPa, and a resilience of up to 86.9%. This range of properties is comparable to the properties of native human arteries and some collagen and fibrinogen-based scaffolds admitting high potential for biomedical applications [77].

A single recombinant honey bee silk protein, namely, AmelF3, has been electrospun successfully into submicro- and nanofibers [78]. For the spinning process, an aqueous solution of the ~30-kDa fibroin AmelF3 was prepared using 3% SDS to solubilise the protein. Dodecyl sulphate was removed in a precipitation process and the silk solution concentrated up to 12.5% (w/v). The pure silk solution could not be spun into fibres as no jet formed from the Taylor cone during the electrospinning process. Only upon the addition of polyethylene oxide (PEO) (900 kDa) that fibres could be formed. At concentrations below 0.5% (w/v), fibres frequently were beaded and generally not uniform. Just upon the addition of 0.67–1.0% (w/v), PEO uniform fibres formed (Figure 5A–C). The silk/PEO blend fibres showed a smooth surface and had diameters of around 200 nm. Secondary structure analysis using Fourier transform infrared spectroscopy (FTIR) showed a high α-helical content, which is in accordance with the structure of natural honey bee silk. However, methanol post-treatment led to an increased proportion of β-sheet structures. Moreover, upon submersion of the fibres in methanol, PEO was washed out, the fibre surface became rougher, and the former observed birefringence of the fibres, referable to a highly ordered structure, was lost. The latter indicated that the PEO molecules rather than the silk molecules contributed to the high degree of orientation in the as-spun fibre.

In order to refrain from organic solvents, spinning has been tested from aqueous spinning dopes. SELP-47K has been spun into nano-ribbons from an aqueous solution, yielding an ultimate tensile strength of 30.8 MPa [79]. One beneficial aspect of the absence of any additional external agents is the possibility to incorporate water-soluble agents into these nano-ribbons being unstable in organic solvents. Therefore, possible applications are envisioned in the field of enzymes, protein, or small molecule encapsulation. Fully aqueous approaches for fibre spinning demonstrated that silk-elastin-like polymer solutions can be spun into fibres at concentrations ranging from 5% to 13% (w/v) although the fibre diameters were less homogenous than those spun out of organic solvents [80].

A slightly different approach involved a different ~70-kDa silk-elastin-like protein, composed of repeats of six silk-like blocks, seven elastin-like blocks, and one lysine substituted elastin-like block [81]. Whilst highly

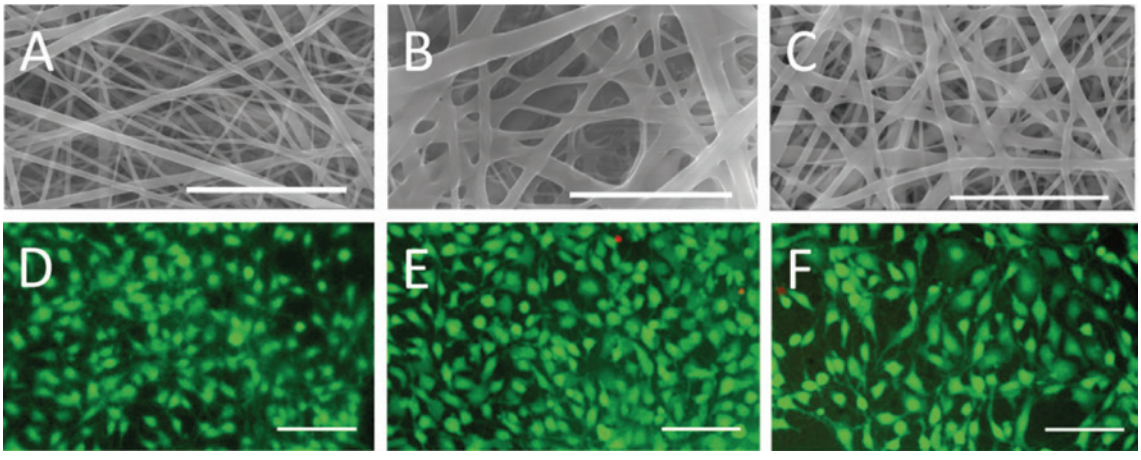

Figure 4: Electrospun SELP-47K mats were tested as scaffolds for fibroblast.
(A)–(C) SEM images of (A) methanol, (B) glutaraldehyde, and (C) methanol and glutaraldehyde treated non-woven mats electrospun from a 15% (w/v) protein solution. Scale bars: 5 μm. (D)–(F) Fluorescent staining for cell viability of fibroblasts grown for 5 days on (D) methanol, (E) glutaraldehyde, and (F) methanol and glutaraldehyde treated SELP-47K scaffolds. Living cells exhibited green, dead cells, red fluorescence. Scale bars: 50 μm. Reprinted and adapted with permission from [77], copyright 2010 American Chemical Society.

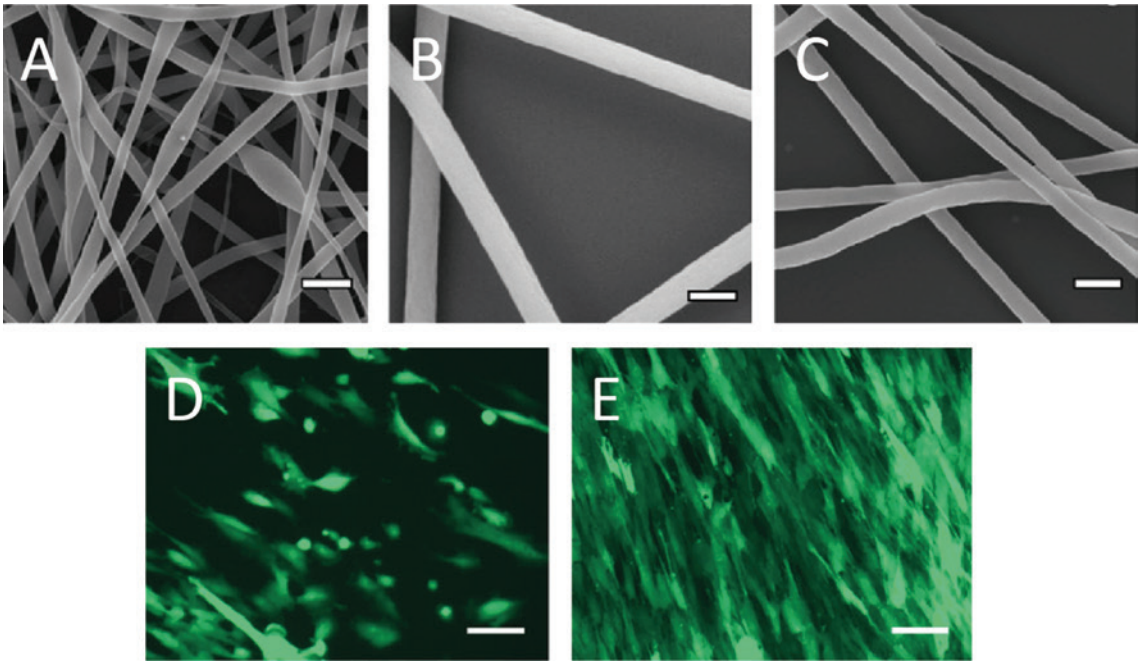

Figure 5: Electrospun fibres made of recombinant honeybee silk and cells cultured on mats made thereof.
(A)–(C) Scanning electron microscopy (SEM) images of fibres from 12.5% AmelF3 protein solutions complemented with (A) 0.4%, (B) 0.67%, and (C) 1% PEO. Scale bars: 500 nm. (D)–(E) Fluorescent images of GFP-expressing fibroblasts grown on electrospun fibre mats for (D) 1 day and (E) 7 days. Scale bars: 100 μm. Reprinted and adapted with permission from [78].

concentrated aqueous solutions of this protein underwent gelation processes, solutions of up to 7% (w/v) did not gel in the timeframe of the experiment. However, they could not be electrospun into fibres. It could be shown that addition of PEO and SDS had several beneficial effects, such as an increase of the viscosity of the spinning solution, a decreased surface tension, as well as an increased electrical conductivity. Together, this would favour the formation of nanofibres. Fibres could be spun successfully upon the addition of 2.1% (w/v) PEO and 1% (w/v) SDS to an aqueous 6.7% (w/v) SELP solution.

Degradability of the electrospun mats by trypsin and α-chymotrypsin revealed the rapid degradation into small peptides without the accumulation of partial degradation products, which renders these fibre mats a highly interesting material for biomaterial applications [78]. Fibroblasts cultivated on electrospun honey bee silk mats adhered and spread well on the material and further proliferated until confluency (Figure 5D–E). It was speculated that the good cell adhesion and proliferation seen on honey bee silk mats might be referred to the similarities regarding the surface chemistry of AmelF3 and collagen, a major protein of the extracellular matrix (ECM).

Synthetic silk-like materials based on combined sequences from *B. mori* fibroin, fibronectin, and elastin have been assessed for cell adhesion and fibre spinning [82]. Two silk-like proteins have been designed: FS_5 containing an RGD motif and FES_8 containing an additional elastin block. Films of the recombinantly produced proteins were assayed for cell adhesion and proliferation. On both protein films, high cell adhesion was reported. However, only FES_8 could be spun into non-woven mats, which was referred to the presence of the elastin block. Due to the good cell-protein film interactions, FES_8 silk mats might be of interest in the field of tissue engineering.

4.2 Films

4.2.1 Methodologies

Silk films or coatings can be produced using a variety of different processing techniques [83] (Figure 6). Films can be produced starting from different (fast-evaporating) organic solvents, acids, or aqueous solutions, e.g. by casting silk solutions into a mould. Upon solvent evaporation, a protein film remains. If highly toxic solvents such as HFIP are used, care must be taken to ensure complete removal of solvent residuals prior to any use as biomaterial. Whilst the high surface-to-volume ratio of fibres obtained by electrospinning methods foster complete solvent evaporation, films cast from solvents may still

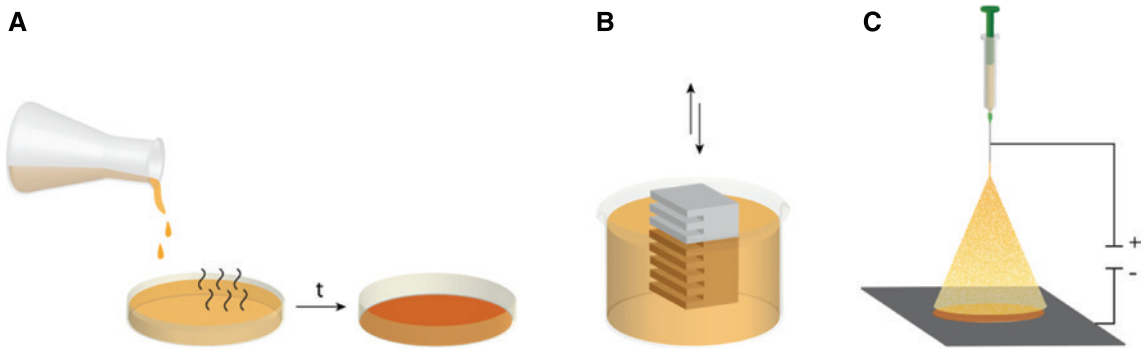

Figure 6: Illustration of different methods of film preparation. (A) Film casting. (B) Dip coating. (C) Electrospraying.

retain small amounts of the solvent. However, in silk films cast from HFIP and post-treated with methanol, no residual HFIP was detectable [84]. Film thickness is mainly determined by the amount of protein. The secondary structure of the silk proteins within the film is highly dependent on the solvent and can therefore be adapted according to the specific needs [83]. Fluorinated solvents such HFIP induce α-helical structure of the silk proteins in the film, whilst films cast from formic acid or from aqueous solutions show high β-sheet content [71, 85, 86]. The silks may be post-treated with ethanol, methanol, other monovalent alcohols, or kosmotropic salt solutions to induce a structural change from α-helical to β-sheet and thereby make the films more stable and water insoluble [87, 88]. If ultra thin films are desired, spin and dip coating may be applied. For the spin-coating process, a droplet of silk solution is applied to the flat substrate. Rotation of the substrate leads to spreading of the silk solution by centrifugal force, and shear forces allow silk proteins to self-assemble [89]. Film thickness can be adjusted by varying, e.g. the silk concentration, viscosity of the solution, or rotational speed. However, one drawback of spin coating is the loss of large amounts of silk solution, as typically, excess solution spun over the boundaries of the substrate cannot be reused. Dip coating allows coating of more complex, three-dimensionally curved surfaces and is mainly conducted with aqueous silk solutions and may be carried out repeatedly. Thin and homogenous films can further be produced by electrospraying of silk solutions. During the spraying process, a fine aerosol with droplets of similar size is produced and, upon deposition of the fine silk droplets on the oppositely charged surface, a homogenous film originates. Importantly, less fast-evaporating solvents are used for electrospraying of films, as a complete evaporation of the solvent has to be avoided as long as the droplet travels to the counter electrode to prevent inadvertent particle formation.

4.2.2 Examples

The recombinant lacewing egg stalk protein $N[AS]_8C$ has been cast into films using formic acid as solvent [54]. Subsequent to solvent evaporation and post-treatment, cells were seeded on these films. Although the protein is positively charged, only poor cell adhesion of fibroblasts and myoblasts was reported on flat $N[AS]_8C$ films [90]. As the topography of films is known to have a significant impact on cells' adhesion behaviour, micro-grooved scaffolds were developed and tested. Structured films of the recombinant lacewing protein $N[AS]_8C$ and a negatively charged, 47-kDa recombinant spider silk protein, eADF4(C16), were prepared with the spider silk protein film forming the ground layer and lacewing silk acting as ridges (Figure 7). The 50-µm broad ridges were arranged in parallel to each other generating grooves of 20 µm in-between them. Cells were seeded on the structured films and analysed for attachment and alignment. Both fibroblasts and myoblasts showed a similar behaviour; few cells adhered on top of the ridges, coinciding with the low cell adhesion on flat $N[AS]_8C$ films, and increased cell adhesion was observed within the grooves. Furthermore, the cells cultured on this surface exhibited a high degree of alignment parallel to the groves. The ability to alter the cell morphology through these patterned films could be interesting in the field of regenerative medicine.

Approaches for the development of vascular grafts have been reported based on recombinant silk fibroin decorated with cell-adhesive sequences produced in transgenic *B. mori* [91]. Laminin and/or fibronectin derived sequences have been fused to silk fibroins, and silk threads of transgenic silkworms were analysed with regard to the incorporation efficiency of the modified silk proteins. It could be shown that only 0.8–7.2% (w/w) of the silk fibroin was modified. Cell culture experiments with films produced from the recombinant silk revealed

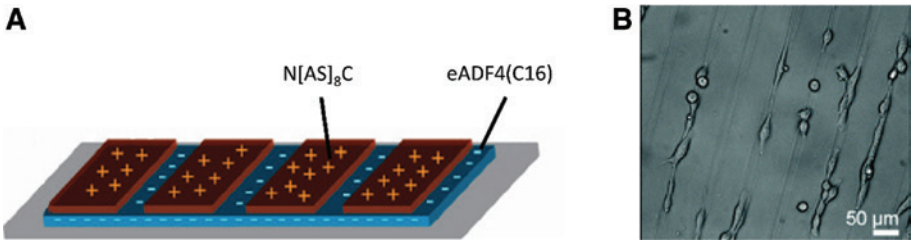

Figure 7: Structured films of recombinant lacewing silk protein N[AS]$_8$C and spider silk protein eADF4(C16).
(A) Scheme depicting the negatively charged eADF4(C16) film as a ground layer for the positively charged N[AS]$_8$C ridges. (B) Light microscopic image of BALB/3T3 fibroblasts cultivated on structured films for 48 h showing mainly aligned orientation along the grooves. Reprinted and adapted with permission from [90].

an increased cell adhesion of mouse endothelial cells as well as smooth muscle cells on silk films upon integration of the laminin sequence, independent if incorporated into light or heavy chain fibroin, and therefore showing potential for these silks to be used as vascular graft material.

Another approach to improve the cell-adhesion on recombinant *B. mori* silk films pursued the insertion of genetically engineered fibroin light chains modified with partial sequences of collagen or fibronectin into the genome of *B. mori* [92]. Cocoon silk of transgenic silkworms was harvested, and films of the recombinant silks were cast from aqueous solutions subsequent to sericin removal from the cocoons. Investigations observing the adhesion of fibroblast cells revealed a significantly improved adhesion on films made of fibroin modified with the collagen-derived sequence and even higher adhesion on films of fibroin modified with the fibronectin-derived sequence containing the RGD motif. Importantly, the amount of recombinant silk in the cocoon silk was very low (below 1% (w/w)). In order to augment the proportion of recombinant silk in the final silk fibre, transgenic silkworms were backcrossed to an Nd-s^D mutant, thereby increasing the production of modified fibroin light chain protein to 3.4% (w/w) of the fibroin. Cell-adhesion activity on this silk was even further increased up to six-fold compared to that on unmodified silk.

Recombinant Vssilk1–4 from the yellow hornet was also processed into films [93]. Cell adhesion experiments showed an increased adhesion of fibroblasts on Vssilk 1 and 2 compared to the remaining two Vssilk proteins, which was referred to the positive net charge of the films under physiological conditions. In further experiments, Vssilk1 was modified carboxy terminally with the RGDS motif and cast into films [94]. Murine fibroblasts cultivated on these Vssilk1-RGDS films showed spread morphologies compared to mainly round shaped cells on Vssilk1 films. Owing to the good solubility of hornet silks and the possibility to produce films with high transparency and flexibility, hornet silk films have great potential for various applications as a biomaterial.

An equimolar mix of the four honey bee silk proteins AmelF1-4 was cast into a film and investigated concerning secondary structure content using FTIR [49]. Native honeybee silk (washed in chloroform to remove wax) contained approximately 65% of coiled-coil structure, and the film cast from the recombinant silk exhibited similar values. Methanol treatment led to secondary structure conversion into β-sheet structures and caused a drop in coiled-coil structure to 48%. It could be shown that films of recombinant honey bee silk can be used for the immobilisation of sensors for the detection of nitric oxide (NO) [95]. Such sensors are relevant for a broad range of applications, like the early prediction of asthma attacks or for the monitoring of industrial pollutants [96, 97]. To produce a heme protein based biosensor, myoglobin was embedded into transparent honey bee silk films cast out of HFIP solution and post-treated with 70% (v/v) methanol. The films were cast on either side of a cuvette, and NO binding was observed by a shift in UV-Vis absorption. Results revealed that myoglobin immobilised on the silk film had a high affinity for NO (K_D of 52 µM), comparable to that of myoglobin in solution (K_D of 30 µM), and therefore could be exploited to detect dissolved NO in concentrations as low as 5 µM. Secondary structure analysis by FTIR revealed no significant differences upon incorporation of myoglobin into the silk films, indicating no disruption of the silk film structure. As a result of the high stability of the myoglobin-silk film, storage was possible as a dry film for at least 60 days, which might also be beneficial for the monitoring of NO levels in the gas phase, e.g. in exhaled breath. NO levels have been shown to increase from less than 5 ppbv (parts per billion by volume) to 20–80 ppbv by airway inflammation [98, 99]. Strikingly, by using these myoglobin-silk films, NO could also be detected in gaseous samples, when 5 ppm was passed through an anaerobic cuvette. Improvements of these films towards

a more sensitive and eventually more selective system to detect gaseous NO would pave the way for their use as an effective, environmentally friendly, and biodegradable biosensor.

De novo engineering of solid-state metalloproteins using a recombinant coiled-coil protein of honey bee larvae has also been reported [100]. Metalloproteins function as enzymes, as transport and storage proteins, or as signal transduction proteins and contain a metal ion as cofactor to allow sophisticated chemistry such as redox reactions. The silk protein AmelF3 has been examined as scaffold for metalloprotein engineering to mimic heme containing proteins. Heme proteins show diverse functions all relying on a common iron porphyrin ring. As the reactivity of naturally occurring heme proteins is determined by direct coordination of the metal ion by an amino acid residue, and interaction of the metal centre and the protein scaffold environment attracts growing attention, both binding and direct coordination of the heme cofactors to the honey bee silk protein were investigated [100]. Notably, if heme *b* solution diffused into an AmelF3 silk film, a colour change of the heme solution from green to red was observed, indicating a change in the coordination of the iron metal centre of the heme group. UV-vis spectroscopy further confirmed the coordination of the heme centre to AmelF3 by a shift in the characteristic Soret peak at ~400 nm. Results obtained from Raman spectroscopy of AmelF3 (sponges) pointed towards the importance of a tyrosine residue, and as AmelF3 only contains one tyrosine (Tyr76), this amino acid was mutated to alanine to confirm the hypothesis that Tyr76 was the coordinating residue. Indeed, a shift in the Soret peak was observed, indicating that the iron centre was not coordinated by the mutated silk protein. It was further reported that in addition to the coordinating tyrosine, the molecular structure of AmelF3 plays an important role, as strong interactions of heme molecules with the honey bee silk were observed whilst *B. mori* cocoon silk absorbed green heme *b* solution, which was then readily washed out with methanol. To investigate the catalytic potential of solid-state metalloproteins, a heterogeneous catalyst was engineered. The catalytic activity of heme *b*-silk materials was assessed using the oxidative coupling of phenol with 4-aminoantipyrine to produce a pink quinone. The increasing absorption at 510 nm indicated the catalytic activity of heme *b*-silk films, whilst silk film controls exhibited no activity (Figure 8).

Varying macrocycles integrated into biosynthetic silk films allows the production of bioinorganic materials that can undergo spin-forbidden singlet-triplet transitions [101]. Heavy-metal macrocycles, e.g. zink phthalocyanine

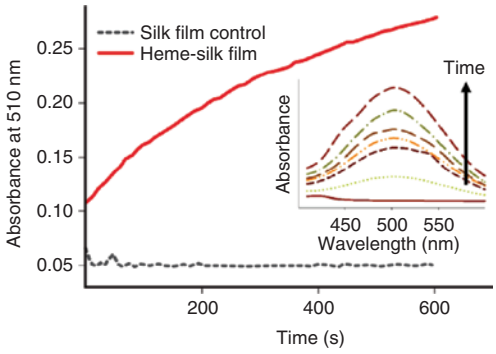

Figure 8: Catalytic activity of a heme *b*-AmelF3 film. Coupling of phenol to 4 amino-antipyrine gives a coloured quinone. The inset shows the change in the solution UV/vis spectrum over time. Reprinted and adapted from [100] under Creative Common Licence.

tetrasulfonate (ZnPcTs), were immobilised on recombinant honey bee silk. Upon excitation using visible light, they are known to undergo crossing from singlet to triplet state. This spin-forbidden transition causes phosphorescence and further leads to the production of cytotoxic oxygen species. Therefore, these constructs represent a versatile material exhibiting antimicrobial activity [101].

Optically transparent films have been produced from the recombinant silk-elastin-like protein SELP-47K [102]. Films with a thickness of 20–100 µm have been cast from aqueous solution and examined for transparency. These thin films exhibited outstanding transmittance from 350 to 800 nm, which was reduced moderately upon crosslinking with glutaraldehyde to stabilise the films. In contrast, methanol treatment retained the transparency of the films. Further, these films were examined for their prospects as drug delivery matrix [103]. Ciprofloxacin, a commonly used antibiotic for the treatment of ocular infections, was used to test the SELP-47K films' suitability. Silk solutions were mixed with the antibiotic prior to film casting, and the release of the drug from the film was investigated over time. Release kinetics varied upon post-treatment of the films with alcohols, probably due to the changed interaction between the drug and the structure of the polymer chains. Drug-loaded silk films released the antibiotic drug for up to 132 h. Additional coating of the drug loaded film with SELP-47K prolonged the drug release up to 220 h. As the incorporation of the drug into the film did not alter its antimicrobial activity, the results showed that optically transparent silk-elastin-like protein films have great potential for the development of novel ophthalmic drug carriers. Therefore, also considering their good performance in in vitro cell culture and drug delivery studies, these films might be suitable for ophthalmic applications,

such as contact lenses, synthetic corneas, or intraocular lenses.

4.3 Hydrogels

4.3.1 Methodologies

Hydrogels are a promising class of materials as they have characteristics similar to those of soft tissues concerning their mechanics and therefore may act as scaffolds in tissue regeneration. Hydrogels are three-dimensional networks of hydrophilic polymers, which swell under considerable increase of volume without dissolution. Hydrogels have been produced from a range of natural and synthetic materials. Generally, gelation occurs upon crosslinking of the polymer chains either chemically, e.g. by addition of chemical reagents such as cross-linkers, or physically, e.g. by application of physical stimulants such as temperature or pH. Interestingly, in vitro, aqueous solutions of silk fibroin undergo a self-assembly based sol-gel transition to form hydrogels, whereby increased protein concentration leads to increased compressive strength of the hydrogel [104]. For silk fibroin solutions (up to 15% (w/v)), the gelation time has been reported to be from days to weeks. For many cell-based applications, a faster gelation process is necessary. The gelation process of aqueous silk fibroin solutions can be accelerated, e.g. by altering the hydrophobic hydration of the silk molecules by ultrasonication [105] or by vortexing [106], whereby a shear-induced transition occurs from a low-viscosity aqueous silk solution with mainly random coil conformation to a β-sheet-rich structure forming a rigid hydrogel. Permanent physical crosslinking leads to a change of the viscoelastic properties of the silk, i.e. an increase in viscosity resulting in an increased complex shear modulus [105]. As the gelation kinetics are dependent on temperature, protein concentration, pH, ions (such as Ca^{2+}), and applied shear, the process can be well controlled [106]. SELPs also form hydrogels. They undergo an irreversible sol-gel transition in a temperature-dependent manner presumably by formation of hydrogen bonds between the silk blocks [58]. The number of silk-like and elastin-like blocks determines the macromolecular properties of the material, and therefore, adequate design of SELP copolymers enables sol-gel transition at physiological conditions. Especially if encapsulation of cells within a hydrogel is envisioned, control over the gelation kinetics during hydrogel formation is important to ensure hydrogel homogeneity as well as to avoid cell sedimentation. Hydrogels are further attractive materials for 3D printing. However, whilst spider silk hydrogels show distinct shape fidelity, plotting of silkworm fibroin based bioinks often requires additives or post-processing [107].

4.3.2 Examples

Drugs and even cells can be trapped within a hydrogel silk matrix. Injectable hydrogels could be used as drug and DNA release systems with controllable release profiles [108]. SELP hydrogels e.g. have been investigated for controlled release of plasmid DNA. Therefore, the influence of hydrogel geometry and molecular weight of plasmid DNA was assessed [109]. It was reported that the effective diffusivity and the release of plasmid DNA were directly dependent on the size of the plasmid. An inverse correlation was found for the average release and the plasmid size ranging from 2.6 to 11 kbp. Further, the conformation of the plasmid was important, as the release rate decreased from linear to supercoiled to open circular. Importantly, the bioactivity of DNA was retained in vitro for up to 28 days, and also bioactive adenoviral vectors could be released rendering this system interesting for both non-viral and viral gene delivery.

Using SELP-47K hydrogels, especially the influence of SELP concentration, curing time, ionic strength of the buffer, and DNA concentration were investigated on the release profile of an approximately 2.6-MDa plasmid [108]. Hydrogel concentrations of 8% and 12% (w/w) containing 50–250 μg/ml plasmid DNA were cured for 1 or 4 h and incubated in release buffer with ionic strengths ranging from 0.03 to 0.5 M. Interestingly, the DNA release profile was not affected by variation of plasmid concentration, whereas curing time, SELP concentration, and especially ionic strength of the release buffer had a great influence. At pH 7.4, the primary amines of lysine and arginine residues found in SELP-47K were considerably protonated and therefore potentially interacted with the negatively charged phosphates of nucleic acids. With increasing ionic strength, counter ions increasingly weakened the plasmid-polymer interactions and consequently led to the release of DNA from the hydrogel matrix. Increasing the hydrogel curing time led to the formation of a denser polymer network resulting in a retarded DNA release, and similarly, increasing the polymer concentration caused a higher cross-linking density and decreased the mean pore size, yielding a delayed DNA release from the matrix. Further studies on DNA and adenovirus release from SELP hydrogels revealed the negative correlation between release, protein concentration, and hydrogel curing time [110, 111].

SELP-47K hydrogels have been investigated for encapsulation and chondrocytic differentiation of human mesenchymal stem cells (hMSCs) to develop an injectable matrix for the delivery of cell-based therapeutics [112]. In order to encapsulate cells, an 11.5% SELP solution was mixed with hMSCs and gelled at 37 °C for 1 h. The encapsulated cells were cultured in chondrogenic medium in the absence or presence of the transforming growth factor TGF-β3. Concerning the cell viability, hMSCs remained metabolically active during cultivation for up to 4 weeks independent of the addition of TGF-β3. Although the cells showed a rounded morphology, cells cultured in the presence of TGF-β3 were embedded in a chondrocytic extracellular matrix as examined by immunohistochemical means. Hence, the previously undifferentiated cells had produced a cartilage-specific matrix. This was further confirmed by investigations on gene expression patterns. hMSCs cultured in the presence of TGF-β3 exhibited an upregulation of chondrogenic markers, such as type II and type X collagen and SOX9 (a transcription factor involved in chondrocyte differentiation) whilst transcription levels of these genes were low in cells cultured in the absence of the growth factor. Thus, SELP-47K hydrogels represent a promising scaffold for the encapsulation of cells, and as chondrogenesis can be enhanced in vitro by the addition of a chondrogenic growth factor, they may find application as therapeutics in cartilage regeneration.

Implementation of (reversible) response mechanisms of SELP hydrogels to stimuli such as pH, temperature, redox state, or ionic strength was achieved by introducing modifications into individual SELP blocks. SELPs with different ratios of silk-to-elastin blocks were synthesised containing periodic cysteine residues within the elastin blocks [113]. The resulting cysteine containing hydrogels were thermally responsive in solution, and hydrogel formation occurred at body temperature under mild oxidative conditions. The mechanical properties could be varied upon varying the silk-to-elastin ratio. Oxidation of cysteine residues led to inter- and intramolecular disulphide bridges creating a covalent supramolecular network. This could further be exploited to release polar model drugs in a redox-sensitive manner. It could be shown that the release of Rhodamine B from Rhodamine B-loaded hydrogels was enhanced significantly upon addition of a reducing reagent.

In another approach, a matrix metalloproteinase (MMP)-sensitive sequence (GPQGIFGQ) was inserted into a SELP, namely, SELP815K, to mediate sensitivity against MMPs, which are known to be overexpressed in tumour tissues, with the goal to release e.g. adenoviral vectors [114]. An increased degradation rate was reported in vitro for both soluble proteins and hydrogels made thereof, whereby the degradation rate of hydrogels was dependent on the site of sequence insertion within the SELP sequence, which was attributed to the higher order structure of the hydrogel matrix and the variation in accessibility of the recognition site. Further in vivo studies investigating the MMP-sensitive hydrogels as matrix for viral gene therapy of head and neck squamous cell carcinoma bearing mice revealed a prolonged survival rate of mice treated with 8% hydrogels if the MMP-sensitive sequence was inserted in the elastin blocks or at the boarder of silk and elastin blocks.

5 Conclusion and outlook

Insect silks represent a highly diverse class of materials produced by a broad range of insects for various applications. Different types of silks with fundamentally different protein structures have evolved and, as a result of evolutionary pressure, have been perfectly adapted to fulfil their respective task. Silk proteins perform in all kinds of environments: honey bees produce silk that performs in the waxen environment of the bee hive; aquatic insects, like caddisfly larvae, produce a highly post-translationally modified silk functioning as underwater adhesive; and many terrestrial insects use their silk as cocoon material. The diversity found in nature might provide a natural blueprint for the development of a great number of green polymer materials for various applications.

However, silks have to compete with other (bio) polymers, and development and approval of materials for biomedical applications are time consuming. Further, for some silks, biotechnological production is difficult, as seen for protein-based underwater adhesives of, e.g. caddisfly silks. Noteworthy, proteins produced in *E. coli* ("white" biotechnology) carry no post-translational modifications, re-emphasising the need of suitable expression hosts for heterologous gene expression. Therefore, either work-arounds have to be identified or new scalable expression hosts (including e.g. plants ("green" biotechnology) or transgenic insects ("yellow" biotechnology)) have to be identified.

In the last decades, great efforts have been made to study silk-producing animals and the properties of their silks and to identify the underlying gene and protein sequences. For the recombinant silk production both, the original sequence as well as the structure-to-function correlation has been of particular interest to facilitate recombinant silk production, either by production of full-length

proteins in appropriate hosts or by mimicking fundamental motifs conferring strength and elasticity to the material. The ease of modifications on the genetic level allows modifications with functional peptides or recognition sequences implementing further possible variations into the material. The combination of mechanical properties of silks, their biocompatibility and the benefit of being an environmentally friendly, biodegradable biopolymer together with the possibility to process silks into a plethora of morphologies renders them highly promising materials for sustainable applications in the near future.

Acknowledgement: This work was supported by the EU-project "Grüne biobasierte Polymere" ("Green biobased polymers") of the District Government of Upper Franconia, European Union EFRE Ziel ETZ Freistaat Bayern – Tschechien (project number 123). We thank Elise DeSimone for proof-reading.

References

1. Scheibel T, Zahn H, Krasowski A. Silk. In: Ullmann's encyclopedia of industrial chemistry. Wiley-VCH Verlag GmbH & Co. KGaA, 2016.
2. Heim M, Keerl D, Scheibel T. Spider silk: from soluble protein to extraordinary fiber. Angewandte Chemie 2009;48:3584–96.
3. Scheibel T. Spider silks: recombinant synthesis, assembly, spinning, and engineering of synthetic proteins. Microbial Cell Factories 2004;3:14.
4. Altman GH, Diaz F, Jakuba C, Calabro T, Horan RL, Chen J, et al. Silk-based biomaterials. Biomaterials 2003;24:401–16.
5. Craig CL. Evolution of arthropod silks. Annu Rev Entomology 1997;42:231–67.
6. Sutherland TD, Young JH, Weisman S, Hayashi CY, Merritt DJ. Insect silk: one name, many materials. Annu Rev Entomol 2010;55:171–88.
7. Weisman S, Trueman HE, Mudie ST, Church JS, Sutherland TD, Haritos VS. An unlikely silk: the composite material of green lacewing cocoons. Biomacromolecules 2008;9:3065–9.
8. Parker KD, Rudall KM. The silk of the egg-stalk of the green lace-wing fly: structure of the silk of Chrysopa egg-stalks. Nature 1957;179:905–6.
9. Vollrath F. Strength and structure of spiders' silks. J Biotechnol 2000;74:67–83.
10. Lang G, Herold H, Scheibel T. Properties of engineered and fabricated silks. In: Parry DA, Squire JM, editors. Fibrous proteins: structures and mechanisms. Cham: Springer International Publishing, 2017.
11. Becker N, Oroudjev E, Mutz S, Cleveland JP, Hansma PK, Hayashi CY, et al. Molecular nanosprings in spider capture-silk threads. Nat Mater 2003;2:278–83.
12. Dicko C, Knight D, Kenney JM, Vollrath F. Secondary structures and conformational changes in flagelliform, cylindrical, major, and minor ampullate silk proteins. Temperature and concentration effects. Biomacromolecules 2004;5:2105–15.
13. Andersson M, Johansson J, Rising A. Silk spinning in silkworms and spiders. Int J Mol Sci 2016;17:E1290.
14. Bini E, Knight DP, Kaplan DL. Mapping domain structures in silks from insects and spiders related to protein assembly. J Mol Biol 2004;335:27–40.
15. Huemmerich D, Scheibel T, Vollrath F, Cohen S, Gat U, Ittah S. Novel assembly properties of recombinant spider dragline silk proteins. Curr Biol CB 2004;14:2070–4.
16. Rudall KM. Silk and other cocoon proteins. In: Florkin M, Mason HS. Comparative biochemistry. New York: Academic Press, 1962.
17. Kenchington W. The larval silk of *Hypera* spp. (Coleoptera: Curculionidae). A new example of the cross-beta protein conformation in an insect silk. J Insect Physiol 1983;29:355–61.
18. Walker AA, Church JS, Woodhead AL, Sutherland TD. Silverfish silk is formed by entanglement of randomly coiled protein chains. Insect Biochem Mol Biol 2013;43:572–9.
19. Atkins ED. A four-strand coiled coil model for some insect fibrous proteins. J Mol Biol 1967;24:139–41.
20. Sutherland TD, Weisman S, Walker AA, Mudie ST. The coiled coil silk of bees, ants, and hornets. Biopolymers 2012;97:446–54.
21. Woolfson DN. The design of coiled-coil structures and assemblies. Adv Protein Chem 2005;70:79–112.
22. Sutherland TD, Weisman S, Trueman HE, Sriskantha A, Trueman JW, Haritos VS. Conservation of essential design features in coiled coil silks. Mol Biol Evol 2007;24:2424–32.
23. Walker AA, Holland C, Sutherland TD. More than one way to spin a crystallite: multiple trajectories through liquid crystallinity to solid silk. Proc Biol Sci 2015;282:20150259.
24. Rudall KM, Kenchington W. Arthropod silks: the problem of fibrous proteins in animal tissues. Annu Rev Entomol 1971;16:73–96.
25. Iizuka E. Silk thread: mechanism of spinning and its mechanical properties. J Appl Polym Sci 1985;41:173–85.
26. Foo CW, Bini E, Hensman J, Knight DP, Lewis RV, Kaplan DL. Role of pH and charge on silk protein assembly in insects and spiders. Appl Phys A 2006;82:223–33.
27. Iizuka E. Properties of the liquid crystals of some biopolymers. Adv Biophys 1988;24:1–56.
28. Akai H. The structure and ultrastructure of the silk gland. Experientia 1983;39:443–9.
29. Magoshi J, Magoshi Y, Nakamura S. Mechanism of fiber formation of silkworm. In: Kaplan D, Wade Adams W, Farmer B, Viney C, editors. Silk polymers. ACS Symposium Series, Vol. 544. Washington: American Chemical Society, 1993:292–310.
30. Domigan LJ, Andersson M, Alberti KA, Chesler M, Xu Q, Johansson J, et al. Carbonic anhydrase generates a pH gradient in Bombyx mori silk glands. Insect Biochem Mol Biol 2015;65:100–6.
31. Sehnal F, Zurovec M. Construction of silk fiber core in lepidoptera. Biomacromolecules 2004;5:666–74.
32. Yonemura N, Mita K, Tamura T, Sehnal F. Conservation of silk genes in Trichoptera and Lepidoptera. J Mol Evol 2009;68:641–53.
33. Hagn F, Thamm C, Scheibel T, Kessler H. pH-dependent dimerization and salt-dependent stabilization of the N-terminal domain of spider dragline silk–implications for fiber formation. Angewandte Chemie 2011;50:310–3.
34. Hagn F, Eisoldt L, Hardy JG, Vendrely C, Coles M, Scheibel T, et al. A conserved spider silk domain acts as a molecular switch that controls fibre assembly. Nature 2010;465:239–42.
35. He YX, Zhang NN, Li WF, Jia N, Chen BY, Zhou K, et al. N-Terminal domain of Bombyx mori fibroin mediates the assembly of silk in response to pH decrease. J Mol Biol 2012;418:197–207.

36. Holland C, Terry AE, Porter D, Vollrath F. Comparing the rheology of native spider and silkworm spinning dope. Nat Mater 2006;5:870–4.
37. Laity PR, Gilks SE, Holland C. Rheological behaviour of native silk feedstocks. Polymer 2015;67:28–39.
38. Asakura T, Umemura K, Nakazawa Y, Hirose H, Higham J, Knight D. Some observations on the structure and function of the spinning apparatus in the silkworm Bombyx mori. Biomacromolecules 2007;8:175–81.
39. Vollrath F, Knight DP. Liquid crystalline spinning of spider silk. Nature 2001;410:541–8.
40. Holland C, Vollrath F, Ryan AJ, Mykhaylyk OO. Silk and synthetic polymers: reconciling 100 degrees of separation. Adv Mater 2012;24:105–9, 4.
41. Flower NE, Kenchington W. Studies on insect fibrous proteins: the larval silk of Apis, Bombus and Vespa (Hymenoptera: Aculeata). J R Microscopical Soc 1967;86:297–310.
42. Silva-Zacarin EC, Silva De Moraes RL, Taboga SR. Silk formation mechanisms in the larval salivary glands of Apis mellifera (Hymenoptera: Apidae). J Biosci 2003;28:753–64.
43. Vendrely C, Scheibel T. Biotechnological production of spider-silk proteins enables new applications. Macromol Biosci 2007;7:401–9.
44. Tsuzuki S, Iwami M, Sakurai S. Ecdysteroid-inducible genes in the programmed cell death during insect metamorphosis. Insect Biochem Mol Biol 2001;31:321–31.
45. Sekimoto T, Iwami M, Sakurai S. Coordinate responses of transcription factors to ecdysone during programmed cell death in the anterior silk gland of the silkworm, Bombyx mori. Insect Mol Biol 2006;15:281–92.
46. Terashima J, Yasuhara N, Iwami M, Sakurai S. Programmed cell death triggered by insect steroid hormone, 20-hydroxyecdysone, in the anterior silk gland of the silkworm, Bombyx mori. Dev Genes Evol 2000;210:545–58.
47. Suzuki Y, Suzuki E. Quantitative measurements of fibroin messenger RNA synthesis in the posterior silk gland of normal and mutant Bombyx mori. J Mol Biol 1974;88:393–407.
48. Sutherland TD, Campbell PM, Weisman S, Trueman HE, Sriskantha A, Wanjura WJ, et al. A highly divergent gene cluster in honey bees encodes a novel silk family. Genome Res 2006;16:1414–21.
49. Weisman S, Haritos VS, Church JS, Huson MG, Mudie ST, Rodgers AJ, et al. Honeybee silk: recombinant protein production, assembly and fiber spinning. Biomaterials 2010;31:2695–700.
50. Sezutsu H, Kajiwara H, Kojima K, Mita K, Tamura T, Tamada Y, et al. Identification of four major hornet silk genes with a complex of alanine-rich and serine-rich sequences in Vespa simillima xanthoptera Cameron. Biosci Biotechnol Biochem 2007;71:2725–34.
51. Shi J, Lua S, Du N, Liu X, Song J. Identification, recombinant production and structural characterization of four silk proteins from the Asiatic honeybee Apis cerana. Biomaterials 2008;29:2820–8.
52. Maitip J, Trueman HE, Kaehler BD, Huttley GA, Chantawannakul P, Sutherland TD. Folding behavior of four silks of giant honey bee reflects the evolutionary conservation of aculeate silk proteins. Insect Biochem Mol Biol 2015;59:72–9.
53. Sutherland TD, Church JS, Hu X, Huson MG, Kaplan DL, Weisman S. Single honeybee silk protein mimics properties of multiprotein silk. PLoS One 2011;6:e16489.
54. Bauer F, Scheibel T. Artificial egg stalks made of a recombinantly produced lacewing silk protein. Angewandte Chemie 2012;51:6521–4.
55. Tanaka K, Kajiyama N, Ishikura K, Waga S, Kikuchi A, Ohtomo K, et al. Determination of the site of disulfide linkage between heavy and light chains of silk fibroin produced by Bombyx mori. Biochim Biophys Acta 1999;1432:92–103.
56. Yamaguchi K, Kikuchi Y, Takagi T, Kikuchi A, Oyama F, Shimura K, et al. Primary structure of the silk fibroin light chain determined by cDNA sequencing and peptide analysis. J Mol Biol 1989;210:127–39.
57. Ohshima Y, Suzuki Y. Cloning of the silk fibroin gene and its flanking sequences. Proc Natl Acad Sci USA 1977;74:5363–7.
58. Cappello J, Crissman JW, Crissman M, Ferrari FA, Textor G, Wallis O, et al. In-situ self-assembling protein polymer gel systems for administration, delivery, and release of drugs. J Controlled Release 1998;53:105–17.
59. Rauscher S, Baud S, Miao M, Keeley FW, Pomes R. Proline and glycine control protein self-organization into elastomeric or amyloid fibrils. Structure 2006;14:1667–76.
60. Muiznieks LD, Keeley FW. Proline periodicity modulates the self-assembly properties of elastin-like polypeptides. J Biol Chem 2010;285:39779–89.
61. Gustafson JA, Ghandehari H. Silk-elastinlike protein polymers for matrix-mediated cancer gene therapy. Adv Drug Delivery Rev 2010;62:1509–23.
62. Spiess K, Ene R, Keenan CD, Senker J, Kremer F, Scheibel T. Impact of initial solvent on thermal stability and mechanical properties of recombinant spider silk films. J Mater Chem 2011;21:13594–604.
63. Gotoh Y, Tsukada M, Baba T, Minoura N. Physical properties and structure of poly(ethylene glycol)-silk fibroin conjugate films. Polymer 1997;38:487–90.
64. Vasconcelos A, Freddi G, Cavaco-Paulo A. Biodegradable materials based on silk fibroin and keratin. Biomacromolecules 2008;9:1299–305.
65. Chen X, Cai H, Ling S, Shao Z, Huang Y. Conformation transition of Bombyx mori silk protein monitored by time-dependent fourier transform infrared (FT-IR) spectroscopy: effect of organic solvent. Appl Spectrosc 2012;66:696–9.
66. Heidebrecht A, Scheibel T. Recombinant production of spider silk proteins. Adv Appl Microbiol 2013;82:115–53.
67. Doblhofer E, Heidebrecht A, Scheibel T. To spin or not to spin: spider silk fibers and more. Appl Microbiol Biotechnol 2015;99:9361–80.
68. Greiner A, Wendorff JH. Electrospinning: a fascinating method for the preparation of ultrathin fibers. Angewandte Chemie 2007;46:5670–703.
69. Reneker DH, Yarin AL. Electrospinning jets and polymer nanofibers. Polymer 2008;49:2387–425.
70. Pan H, Li L, Hu L, Cui X. Continuous aligned polymer fibers produced by a modified electrospinning method. Polymer 2006;47:4901–4.
71. Stephens JS, Fahnestock SR, Farmer RS, Kiick KL, Chase DB, Rabolt JF. Effects of electrospinning and solution casting protocols on the secondary structure of a genetically engineered dragline spider silk analogue investigated via Fourier transform Raman spectroscopy. Biomacromolecules 2005;6:1405–13.

72. Bauer F, Bertinetti L, Masic A, Scheibel T. Dependence of mechanical properties of lacewing egg stalks on relative humidity. Biomacromolecules 2012;13:3730–5.
73. Poole J, Church JS, Woodhead AL, Huson MG, Sriskantha A, Kyratzis IL, et al. Continuous production of flexible fibers from transgenically produced honeybee silk proteins. Macromol Biosci 2013;13:1321–6.
74. Huson MG, Church JS, Poole JM, Weisman S, Sriskantha A, Warden AC, et al. Controlling the molecular structure and physical properties of artificial honeybee silk by heating or by immersion in solvents. PLoS One 2012;7:e52308.
75. Hepburn HR, Chandler HD, Davidoff MR. Extensometric properties of insect fibroins - green lacewing cross-beta, honeybee alpha-helical and greater waxmoth parallel-beta conformations. Insect Biochem 1979;9:69–77.
76. Qiu W, Teng W, Cappello J, Wu X. Wet-spinning of recombinant silk-elastin-like protein polymer fibers with high tensile strength and high deformability. Biomacromolecules 2009;10:602–8.
77. Qiu W, Huang Y, Teng W, Cohn CM, Cappello J, Wu X. Complete recombinant silk-elastinlike protein-based tissue scaffold. Biomacromolecules 2010;11:3219–27.
78. Wittmer CR, Hu X, Gauthier PC, Weisman S, Kaplan DL, Sutherland TD. Production, structure and in vitro degradation of electrospun honeybee silk nanofibers. Acta Biomater 2011;7:3789–95.
79. Ner Y, Stuart JA, Whited G, Sotzing GA. Electrospinning nanoribbons of a bioengineered silk-elastin-like protein (SELP) from water. Polymer 2009;50:5828–36.
80. Machado R, da Costa A, Sencadas V, Garcia-Arevalo C, Costa CM, Padrao J, et al. Electrospun silk-elastin-like fibre mats for tissue engineering applications. Biomed Mater 2013;8:065009.
81. Nagarajan R, Drew C, Mello CM. Polymer – micelle complex as an aid to electrospinning nanofibers from aqueous solutions. J Phys Chem C 2007;111:16105–8.
82. Yang M, Tanaka C, Yamauchi K, Ohgo K, Kurokawa M, Asakura T. Silklike materials constructed from sequences of Bombyx mori silk fibroin, fibronectin, and elastin. J Biomed Mater Res. Part A 2008;84:353–63.
83. Borkner CB, Elsner MB, Scheibel T. Coatings and films made of silk proteins. ACS Appl Mater Interfaces 2014;6:15611–25.
84. Hardy JG, Leal-Eganã A, Scheibel T. Engineered spider silk protein-based composites for drug delivery. Macromol Biosci 2013;13:1431–7.
85. Zhao C, Yao J, Masuda H, Kishore R, Asakura T. Structural characterization and artificial fiber formation of Bombyx mori silk fibroin in hexafluoro-iso-propanol solvent system. Biopolymers 2003;69:253–9.
86. Ha SW, Tonelli AE, Hudson SM. Structural studies of Bombyx mori silk fibroin during regeneration from solutions and wet fiber spinning. Biomacromolecules 2005;6:1722–31.
87. Huemmerich D, Slotta U, Scheibel T. Processing and modification of films made from recombinant spider silk proteins. Appl Phys A 2006;82:219–22.
88. Slotta U, Tammer M, Kremer F, Koelsch P, Scheibel T. Structural analysis of spider silk films. Supramol Chem 2006;18:465–71.
89. Greving I, Cai M, Vollrath F, Schniepp HC. Shear-induced self-assembly of native silk proteins into fibrils studied by atomic force microscopy. Biomacromolecules 2012;13:676–82.
90. Bauer F, Wohlrab S, Scheibel T. Controllable cell adhesion, growth and orientation on layered silk protein films. Biomater Sci 2013;1:1244–9.
91. Asakura T, Isozaki M, Saotome T, Tatematsu K-i, Sezutsu H, Kuwabara N, et al. Recombinant silk fibroin incorporated cell-adhesive sequences produced by transgenic silkworm as a possible candidate for use in vascular graft. J Mater Chem B 2014;2:7375–83.
92. Yanagisawa S, Zhu Z, Kobayashi I, Uchino K, Tamada Y, Tamura T, et al. Improving cell-adhesive properties of recombinant Bombyx mori silk by incorporation of collagen or fibronectin derived peptides produced by transgenic silkworms. Biomacromolecules 2007;8:3487–92.
93. Kambe Y, Sutherland TD, Kameda T. Recombinant production and film properties of full-length hornet silk proteins. Acta Biomaterialia 2014;10:3590–8.
94. Kambe Y, Kameda T. Production and cell adhesion activity of recombinant full-length hornet silk protein fused with RGDS peptide. J Silk Sci Technol Jpn 2014;22:47–9.
95. Rapson TD, Church JS, Trueman HE, Dacres H, Sutherland TD, Trowell SC. Micromolar biosensing of nitric oxide using myoglobin immobilized in a synthetic silk film. Biosens Bioelectron 2014;62:214–20.
96. Gelb AF, Barnes PJ, George SC, Ricciardolo FL, DiMaria G, Zamel N. Review of exhaled nitric oxide in chronic obstructive pulmonary disease. J Breath Res 2012;6:047101.
97. Sigrist MW. Air monitoring by spectroscopic techniques. New York: Wiley, 1994:560.
98. Yates DH. Role of exhaled nitric oxide in asthma. Immunol Cell Biol 2001;79:178–90.
99. Dweik RA, Boggs PB, Erzurum SC, Irvin CG, Leigh MW, Lundberg JO, et al. An official ATS clinical practice guideline: interpretation of exhaled nitric oxide levels (FENO) for clinical applications. Am J Respir Crit Care Med 2011;184:602–15.
100. Rapson TD, Sutherland TD, Church JS, Trueman HE, Dacres H, Trowell SC. De novo engineering of solid-state metalloproteins using recombinant coiled-coil silk. ACS Biomater Sci Eng 2015;1:1114–20.
101. Horgan CC, Han Y-S, Trueman H, Jackson CJ, Sutherland TD, Rapson TD. Phosphorescent oxygen-sensing and singlet oxygen production by a biosynthetic silk. RSC Adv 2016;6:39530–3.
102. Teng W, Huang Y, Cappello J, Wu X. Optically transparent recombinant silk-elastinlike protein polymer films. J Phys Chem B 2011;115:1608–15.
103. Teng W, Cappello J, Wu X. Physical crosslinking modulates sustained drug release from recombinant silk-elastinlike protein polymer for ophthalmic applications. J Control Release 2011;156:186–94.
104. Kim UJ, Park J, Li C, Jin HJ, Valluzzi R, Kaplan DL. Structure and properties of silk hydrogels. Biomacromolecules 2004;5:786–92.
105. Wang X, Kluge JA, Leisk GG, Kaplan DL. Sonication-induced gelation of silk fibroin for cell encapsulation. Biomaterials 2008;29:1054–64.
106. Yucel T, Cebe P, Kaplan DL. Vortex-induced injectable silk fibroin hydrogels. Biophys J 2009;97:2044–50.
107. Malda J, Visser J, Melchels FP, Jungst T, Hennink WE, Dhert WJ, et al. 25th anniversary article: engineering hydrogels for biofabrication. Adv Mater 2013;25:5011–28.
108. Huang W, Rollett A, Kaplan DL. Silk-elastin-like protein biomaterials for the controlled delivery of therapeutics. Expert Opin Drug Delivery 2015;12:779–91.

109. Megeed Z, Haider M, Li D, O'Malley BW, Jr., Cappello J, Ghandehari H. In vitro and in vivo evaluation of recombinant silk-elastinlike hydrogels for cancer gene therapy. J Control Release 2004;94:433–45.
110. Hatefi A, Cappello J, Ghandehari H. Adenoviral gene delivery to solid tumors by recombinant silk-elastinlike protein polymers. Pharm Res 2007;24:773–9.
111. Dandu R, Ghandehari H, Cappello J. Characterization of structurally related adenovirus-laden silk-elastinlike hydrogels. J Bioact Compatible Polym 2008;23:5–19.
112. Haider M, Cappello J, Ghandehari H, Leong KW. In vitro chondrogenesis of mesenchymal stem cells in recombinant silk-elastinlike hydrogels. Pharm Res 2008;25:692–9.
113. Zhou ML, Qian ZG, Chen L, Kaplan DL, Xia XX. Rationally designed redox-sensitive protein hydrogels with tunable mechanical properties. Biomacromolecules 2016;17:3508–15.
114. Price R, Poursaid A, Cappello J, Ghandehari H. In vivo evaluation of matrix metalloproteinase responsive silk-elastinlike protein polymers for cancer gene therapy. J Control Release 2015;213:96–102.